

# Ordinal patterns in the Duffing oscillator: Analyzing powers of characterization

Cite as: Chaos **31**, 023104 (2021); <https://doi.org/10.1063/5.0037999>

Submitted: 18 November 2020 . Accepted: 11 January 2021 . Published Online: 01 February 2021

Ivan Gunther,  Arjendu K. Pattanayak, and  Andrés Aragonese



[View Online](#)




[Export Citation](#)




[CrossMark](#)





Sign up for topic alerts  
New articles delivered to your inbox



# Ordinal patterns in the Duffing oscillator: Analyzing powers of characterization

Cite as: Chaos 31, 023104 (2021); doi: 10.1063/5.0037999

Submitted: 18 November 2020 · Accepted: 11 January 2021 ·

Published Online: 1 February 2021



View Online



Export Citation



CrossMark

Ivan Gunther,<sup>1,a)</sup> Arjendu K. Pattanayak,<sup>1,a)</sup>  and Andrés Aragonese<sup>2,a)</sup> 

## AFFILIATIONS

<sup>1</sup>Department of Physics and Astronomy, Carleton College, 1 N College St, Northfield, Minnesota 55057, USA

<sup>2</sup>Department of Physics, Eastern Washington University, Cheney, Washington 99004, USA

<sup>a)</sup>Authors to whom correspondence should be addressed: [ivanawg@gmail.com](mailto:ivanawg@gmail.com); [arjendu@carleton.edu](mailto:arjendu@carleton.edu); and [aaaragonese@ewu.edu](mailto:aaaragonese@ewu.edu)

## ABSTRACT

Ordinal patterns are a time-series data analysis tool used as a preliminary step to construct the permutation entropy, which itself allows the same characterization of dynamics as chaotic or regular as more theoretical constructs such as the Lyapunov exponent. However, ordinal patterns store strictly more information than permutation entropy or Lyapunov exponents. We present results working with the Duffing oscillator showing that ordinal patterns reflect changes in dynamical symmetry that is invisible to other measures, even permutation entropy. We find that these changes in symmetry at given parameter values are correlated with a change in stability at *neighboring* parameters, which suggests a novel predictive capability for this analysis technique.

Published under license by AIP Publishing. <https://doi.org/10.1063/5.0037999>

Nonlinear dynamical systems can be regular, stable, and simple as well as chaotic, unstable, and complex and sometimes switch between the two behaviors abruptly as a function of parameters. Among the techniques useful in distinguishing between these very different dynamics is computing the so-called permutation entropy (PE) for the system. Here, the time-series associated with a dynamical observable is first converted into a discrete set of observations about extreme events (maxima or minima, for example), and the relative length of the time-spacing between these events is then used to construct “ordinal patterns” or words. The PE is the entropy associated with the probability distribution of these words. The probability distributions themselves contain strictly more information than does the PE. In our work, we show that the probability distributions of words can be analyzed to discover changes in dynamical symmetry in chaotic regimes (and stable regimes). We show that in fact the growth of symmetry in word probabilities are quantifiably more frequent when the system is about to transition to stable behavior at a nearby parameter, thus allowing for the possibility of predictions beyond that of the usual techniques.

## I. INTRODUCTION

Nonlinear dynamical systems display a rich variety of behaviors. Within such systems, the dynamics can be regular,

repeating periodically where the periodicity can be simple or high-order, or else repeating quasi-periodically. These dynamics can also be stable such that a small perturbation or error in the specification of initial conditions do not grow or qualitatively change the behavior. Long-term predictability is only possible under these circumstances. However, such systems often evolve in a chaotic (bounded and non-periodic) and unpredictable manner such that small errors do grow exponentially rapidly; this is quantified by the existence of a positive definite maximal Lyapunov exponent (LE) of the dynamics that measures the sensitivity to initial conditions and is the inverse time scale for predictability. Chaotic trajectories are algorithmically complex<sup>1</sup> in that any recorded time-series for a given observable cannot be compressed by an arbitrary factor. In contrast, regular systems do not have positive LEs and are algorithmically simple. Typically, we see both kinds of behavior: If there are co-existing attractors, this can occur as a function of initial conditions. In other situations, the dynamics can switch back and forth between the two abruptly as a function of system parameters. The sensitivity to change of parameters can also strongly affect controllability and dynamical response.<sup>2–5</sup>

Since such nonlinear systems are ubiquitous in nature, occurring, for example, in mechanical structures such as bridges and in physiological systems, apart from the wide range of physics applications, identifying the difference between the two kinds of behavior and the possibility of a transition between them can, therefore, be

of literally vital importance. However, LEs are difficult to access in experimental or observational situations since they are a theoretical construct that requires access to the fiducial dynamical trajectory itself *and* its tangent space—that is, its response to infinitesimally small perturbations. Techniques based on extracting the informational complexity directly from experimental observations have been developed over the years to address this challenge.<sup>6–10</sup> In particular, the permutation entropy (PE)<sup>7</sup> computed from the probability distribution of ordinal patterns (or “words,” defined more carefully below) constructed from the time-series has been shown to be a suitable alternative for LEs, particularly, in following parameter dependencies, including applications to semi-classical problems.<sup>11</sup>

Intriguingly, in constructing the PE from ordinal patterns, information is compressed: that is, the probability distributions and, particularly, their dependence on parameters contain more information about the dynamics than the PE such that it is possible to go beyond the simple classification into “chaotic” and “regular.” Thus, ordinal patterns can be helpful in understanding the system’s dynamics in situations involving experimental time-series of known dynamics and changeable parameters,<sup>12–16</sup> where one might seek to understand the structured behavior of the system beyond the existence or lack of chaos or where one might not have access to LEs.

In this paper, we present results from a study of the complex dynamics of the paradigmatic Duffing oscillator aimed at characterizing the information hidden in the probability patterns of words and uncover some potential values for this information. We start from the observation that changes in word frequencies arise from a change in temporal symmetries, which we then capture with symmetry-based characterizations of word probability distributions. Changes in the behavior of these criteria as a function of dynamical parameters are visually observed to be—and then quantifiably correlated with—a chaos-stability transition at *neighboring* parameters, which is one of our main results. When we compare some well known techniques (LEs, PE, Poincaré sections, Fourier spectra of time-series, and phase space diagrams) applied to our system, we do not observe such correlation in these other measures. We then dig further into approaches intended to capture temporal correlations in the time-series to see if the patterns visible in word populations can be understood better. Specifically, we show word probabilities can be derived from Interval Trio Maps (ITMs), a generalization of a return map where the probability distribution of consecutive inter-event intervals is mapped into a higher-dimensional space such that changes in probabilities correspond to change in clustering in sectors of the ITM space. We also consider Generalized Poincaré Sections (GPSs) that can be understood as the projection of the dynamics into a subspace following an event-driven criterion. While these latter new analysis techniques contain novel information complementary to that from other techniques, they provide similar results and also seem to fail to display the correlation seen in word probability distributions. Thus, probability distribution of ordinal patterns not only capture signatures of temporal correlations and memory in complex dynamical systems<sup>12,14,16</sup> but also provide information about the system not available with other techniques, in particular (precursor) signals about qualitative dynamical transitions as a function of the parameter.

Below, we first describe the Duffing oscillator and the known analysis tools we use to study it, focusing, in particular, on the

permutation entropy and ordinal patterns, and present our initial results from scanning parameter space. In Sec. III, we describe the detailed analysis of word populations and introduce the new symmetry-based metrics, the behavior of which we compare to the behavior of the PE and the LE. We then discuss the standard techniques and introduce some new analysis techniques—the GPS and ITM—and compare their results to those from words. We conclude after a short discussion including the potential applicability of these new techniques.

## II. WORDS IN THE DUFFING OSCILLATOR

The Duffing oscillator is a paradigmatic model<sup>17</sup> of a damped and periodically driven nonlinear oscillator, completely characterized by trajectories in a phase-space defined by position, momentum, and time, or  $x[t]$ ,  $p[t] = \dot{x}[t]$ , and  $t$ . We study here the bi-stable version, where the oscillator can, in principle, travel between two potential wells. These dynamics are defined by

$$\ddot{x} + d\dot{x} + ax + bx^3 = g \cos \omega t, \quad (1)$$

where we have chosen default dimensionless constants of stiffness  $a = 1$ , nonlinearity  $b = -1$  and damping  $d = 0.3$ . For the detailed studies we present below, we also fix the external driving frequency at  $\omega = 1.2$  and scan its amplitude  $g$  across a range chosen to show a variety of behaviors. Generically, all results carry into other parameter regimes, even though we do not present them here. In this system’s parameter space, there exist distinct regions or bands of chaos and regularity, where the regularity can arise from global stable attractors that are either simple or high-order periodic orbits. We take care to simulate the dynamics to discard initial transient behavior (though there always remain the possibility of “long transients”) by using simulation runs of  $t = 10\,000$ . This is particularly important, for example, in constructing Lyapunov exponents that we do using the method laid out by Wolf.<sup>6</sup>

To construct words or ordinal patterns, we need to select events in the time-series that characterize the dynamics on some natural time scales. Specifically, from the time-series for the position, we record the time-values of local maxima or “peaks” in  $x(t)$  as the events and record properties of these events, in our case, the lengths of time between peaks or “interpeak intervals.” In this process of selecting specific points in the time-series, we are discarding other, redundant points. A certain amount of data compression is involved, which is important in extracting global patterns that may be invisible in the full data: For example, Poincaré section sample trajectories—usually at natural turning points of the dynamics—and thus reveal periodicity or quasi-periodicity.

Sequences of interpeak intervals determine the words. That is, words are defined by considering groups of  $n$  consecutive or semi-consecutive (where one would skip every other or every third) events in a time-series, which are then ranked within the group according to some selected criteria.<sup>7</sup> In our case, we choose  $n = 3$  so that the words are 3-dimensional (i.e., they are constructed from trios of events), consecutive (not skipping regular events), and rank interpeak intervals. For instance, if the first of three interpeak intervals is of the middling length, the second is the shortest of the three, and the third is the longest, this would be categorized as a “1–0–2” type word so that we have one incident of the word  $w_{102}$ .

It is easy to see that there are thus six types of 3D words:  $w_{012}$ ,  $w_{021}$ ,  $w_{102}$ ,  $w_{120}$ ,  $w_{201}$ , and  $w_{210}$ , whose relative populations across the time-series is the quantity of interest. We choose  $n = 3$  for practical reasons: we can confirm empirically that 2-dimensional words do not yield detailed structure, there being only two types, whereas 4-dimensional and beyond subdivide dynamics too much to be useful. This is another example of judicious choice of information compression being necessary to see patterns. We should also note that marginal cases where two or more intervals in the trio were of equal length within the accuracy of our simulation are recorded as being  $w_{111}$  or periodic words. In what follows, we have excluded periodic words, though depending on the goal of the words analysis, some researchers choose to remove them, add them to another word's population, or treat them as experimental uncertainty; we also note that in our case, they are well-defined and abundant.

Already words have been fruitfully applied to the Duffing oscillator to show that permutation entropy, derived from word populations, tracks chaos and stability much like Lyapunov exponents<sup>7</sup> and detects certain changes in the dynamics that LE cannot.<sup>11</sup> We note that the attempt to find further structure in word populations beyond the PE is not new: For example, Bandt<sup>18,19</sup> has studied spatial 3D words and constructed various functions from their populations, as discussed below.

We start with some initial results from our parameter scan, focusing on varying  $g$  from 0.25 to 0.60 in increments of 0.01; this range shows several transitions between bands of regular to chaotic behavior of relevance to our study. We show here LEs (see Fig. 1), word populations (see Fig. 3), and PE (see Fig. 2), which is calculated from word populations  $P_{w_i}$  for each word  $w_i$  of dimension  $D$  as

$$PE = - \sum_i^D \frac{P_{w_i} \log P_{w_i}}{\log(D!)} \quad (2)$$

This construction makes clear how the PE embodies a compression of information about word populations, whence there is arguably

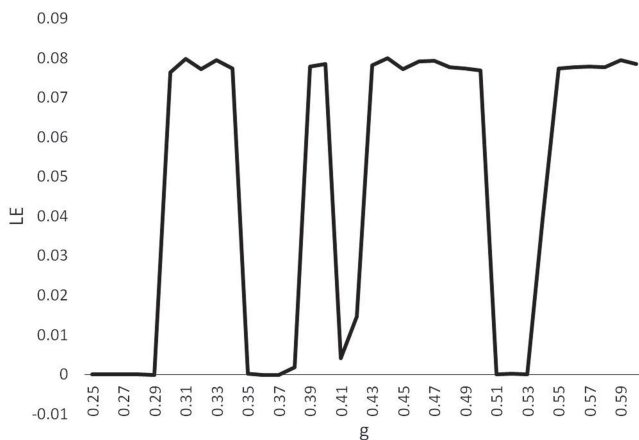


**FIG. 1.** Plot of the Lyapunov exponent as a function of the driving constant  $g$ . At the  $g$ -values of 0.41, 0.42, and 0.54, the chaos is transient, as confirmed by running the oscillator slightly beyond  $t = 10\,000$ .

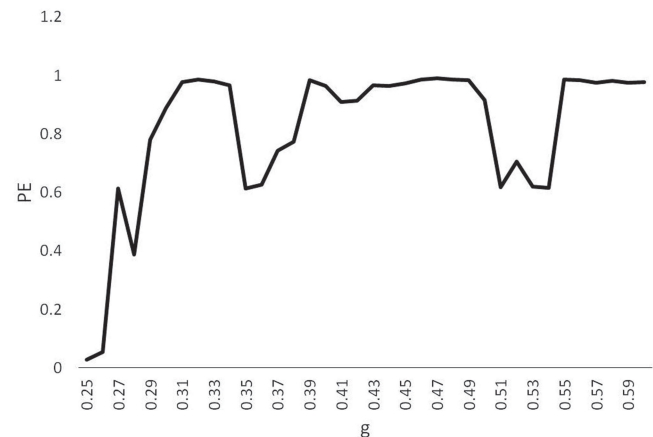


**FIG. 2.** Plot of permutation entropy as a function of  $g$ , calculated from word populations. Note the broad agreement with LE, in that parameters with low LE tend to have permutation entropy below 0.9.

more information about the dynamics in the distribution of words than is visible in the PE. As baselines, we compare the parameter dependence of these quantities with the traditional measure of LEs. These exponents measure the sensitivity to perturbation of the dynamics, and characterize the (exponential) rate at which two slightly different initial conditions separate in phase-space. While the number of Lyapunov exponents depends on the number of dimensions in the dynamics, the focus is typically on the largest, which is positive for a chaotic system. We find indeed that LE and PE scans show the same structure of chaos and stability bands, although their agreement is imperfect in the presence of long transient chaos. We term this behavior as long transient chaos because the dynamics collapse into stability sometime *after*  $t = 10\,000$  time, unlike stable regions which manifest as regular much faster, and fully chaotic regions that remain so for seemingly indefinite times. Long transient chaos at  $g = 0.41 - 0.42$  is nearly indistinguishable from chaos through the PE but at  $g = 0.54$ , the PE treats it as full stability, even though the corresponding LE is higher than at 0.42.

The scan of word populations, on the other hand, stand out from the PE and LE scans. Not only does this follow the transitions from regularity, it also points to the existence of *different* types of chaos (as well as *different* types of stability). For example, compare  $g = 0.32$  with  $g = 0.34$ , which are both chaotic according to both the LE and the PE calculations. However, at  $g = 0.32$ , we find that the word populations are distributed roughly evenly such that their values could be the result of random chance, while at  $g = 0.34$ , the dynamics shows a clear systemic preference for certain three words over certain other three, a preference that becomes even more clear and absolute as the dynamics become stable at  $g = 0.35$ . In fact, this pattern persists in general: word populations seem to become more ordered or structured often in the chaotic regime. Our first observation is that this increase in order seems to happen at parameter values, which are near  $g$  values where stable orbits exist (in this case at  $g = 0.35$ ) that is closer to  $g = 0.34$  than the more disordered  $g = 0.32$ . This and other examples are visible in Fig. 3.

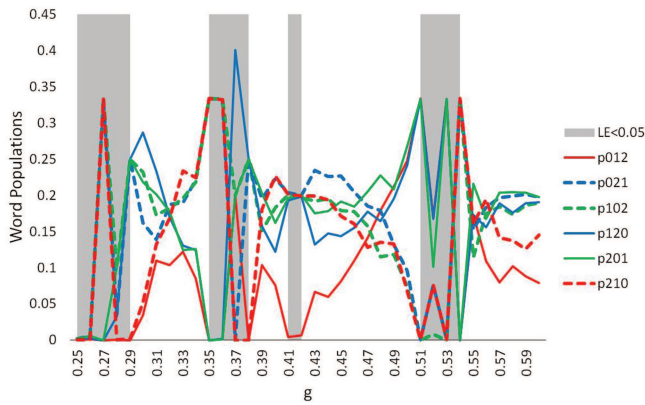


**FIG. 3.** Plot of word populations as a function of  $g$ , with stable or transiently chaotic parameters highlighted in gray. Note that in some cases, the sum of the populations is less than 1, due to an abundance of consecutive interpeak intervals that were nearly exactly equal ( $w_{111}$  not plotted) and, therefore, could not be ordinalized. The  $g$ -values 0.30, 0.34, and 0.50 are chaotic, as shown in Fig. 1, but exhibit certain groupings that mimic their stable neighbors.

These results and, in particular, the changes in the dynamics are still difficult to parse properly. To better clarify the changes that word populations exhibit, we dig deeper using two methods of grouping word populations using “symmetry groups,” which we rigorously quantify and explicate in Sec. III but motivate here. We have chosen these symmetries, as opposed to other inter-word relationships, essentially empirically, based on their apparent prevalence in the observed data (Fig. 3), and their intuitive definitions. The first type of symmetry we consider is *rotational symmetry*, which occurs when the populations of  $w_{012}$ ,  $w_{120}$ , and  $w_{201}$  are similar to each other, as are those of  $w_{021}$ ,  $w_{210}$ , and  $w_{102}$ , but these two population groups are dissimilar to each other. Mathematically, high rotational symmetry is characterized by

$$P_{012} \simeq P_{120} \simeq P_{201} \neq P_{021} \simeq P_{210} \simeq P_{102}. \quad (3)$$

This rotational symmetry is intuitively a *weak* indication of period-3 orbits in the time-series; that is, if each word leads into another in a chain, e.g., 012012012..., we would obtain an equal abundance of  $w_{012}$ ,  $w_{120}$ , and  $w_{201}$ . Since words are ordinal (that is, constructed from a coarse-graining of the time-series), and since the presence of these symmetries is relative but not absolute, it is not an absolute indicator of true period-3 orbits. The second type, *mirror symmetry*, occurs when populations of  $w_{012}$  and  $w_{210}$  are similar, as are those of  $w_{021}$  and  $w_{120}$ , as are those of  $w_{102}$  and  $w_{201}$ , and all three of these pairs are dissimilar to each other. Mathematically, high mirror symmetry would follow from

$$P_{012} \simeq P_{210} \neq P_{021} \simeq P_{120} \neq P_{102} \simeq P_{201}, \quad (4)$$

corresponding to a tendency for small-scale events in the time-series to resemble themselves, regardless of the direction of time. This is a weak form of time-reversal invariance. For example, we see that at  $g = 0.27$  and  $g = 0.35 - 0.36$ , both of which appear only as stable to the LE (Fig. 1), exhibit near-perfect rotational symmetry, wholly different from nearby  $g = 0.29$  and  $g = 0.38$ , which are also simply

stable according to the LE, but in contrast have equal populations of the two mirror symmetry groups and total absence of the third. This symmetry is correlated to differences in the time-series and phase diagrams in the stable regime (Fig. 4). However, similar changes in symmetry do not visibly hold for chaotic phase diagrams. Before we turn to the more detailed discussion of these symmetries in the dynamics, we remark that some types of stability prevent the formation of certain types of words altogether: if the oscillator has perfect period-1 or period-2 orbits, then equality between nearby interpeak intervals will prevent ordinalization of 3D words. This phenomenon is obvious in word population graphics like Fig. 3 because the sum of the six words is significantly less than 1 at these locations, such as at  $g = 0.52$ . This is because during the word-counting process, we designated all marginal cases as “periodic words” or  $w_{111}$ , which counts against the fractional populations of all other words, but which is not shown in Fig. 3.

### III. QUANTIFYING SYMMETRY

We can formalize the notions of the existence of rotational and mirror symmetry groups in the dynamics by computing statistical variances with the average populations  $P_{R1}$ ,  $P_{R2}$ ,  $P_{M1}$ ,  $P_{M2}$ ,  $P_{M3}$ ,  $P_{all}$ , defined below

$$\bar{P}_{R1} = \frac{P_{012} + P_{120} + P_{201}}{3}, \quad (5)$$

$$\bar{P}_{R2} = \frac{P_{210} + P_{021} + P_{102}}{3}, \quad (6)$$

$$\bar{P}_{M1} = \frac{P_{012} + P_{210}}{2}, \quad (7)$$

$$\bar{P}_{M2} = \frac{P_{120} + P_{021}}{2}, \quad (8)$$

$$\bar{P}_{M3} = \frac{P_{201} + P_{102}}{2}, \quad (9)$$

$$\bar{P}_{all} = \frac{P_{012} + P_{021} + P_{102} + P_{120} + P_{201} + P_{210}}{6}. \quad (10)$$

Note that because we omit  $P_{111}$ , it is not necessary that  $\bar{P}_{all} = \frac{1}{6}$ ; hence, we treat the quantity as its own object. We use these average populations and the individual word populations to construct statistical variances that represent symmetry, giving us four measures: rotational variance ( $\psi$ ), rotational hierarchy ( $\Psi$ ), mirror variance ( $\xi$ ), and mirror hierarchy ( $\Xi$ ),

$$\psi = \frac{(P_{012} - \bar{P}_{R1})^2 + (P_{120} - \bar{P}_{R1})^2 + (P_{201} - \bar{P}_{R1})^2}{6} + \frac{(P_{210} - \bar{P}_{R2})^2 + (P_{021} - \bar{P}_{R2})^2 + (P_{102} - \bar{P}_{R2})^2}{6}, \quad (11)$$

$$\Psi = \frac{(\bar{P}_{R1} - \bar{P}_{all})^2 + (\bar{P}_{R2} - \bar{P}_{all})^2}{2}, \quad (12)$$

$$\xi = \frac{(P_{012} - \bar{P}_{M1})^2 + (P_{210} - \bar{P}_{M1})^2 + (P_{120} - \bar{P}_{M2})^2}{6} + \frac{(P_{021} - \bar{P}_{M2})^2 + (P_{201} - \bar{P}_{M3})^2 + (P_{102} - \bar{P}_{M3})^2}{6}, \quad (13)$$

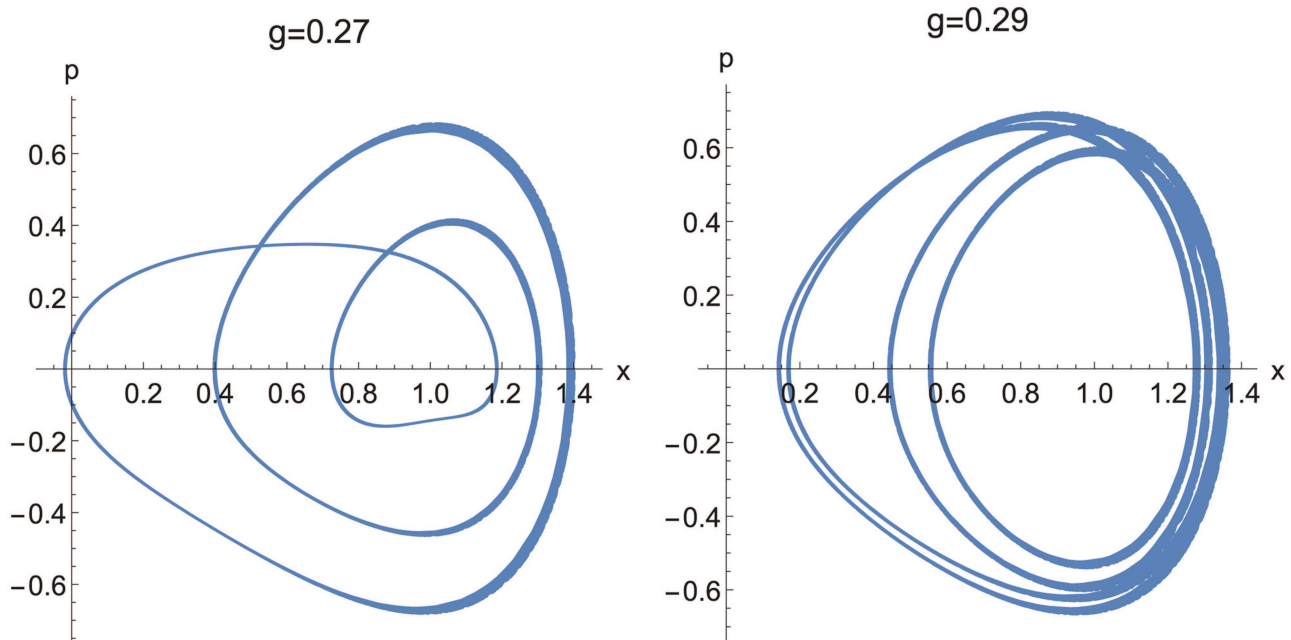


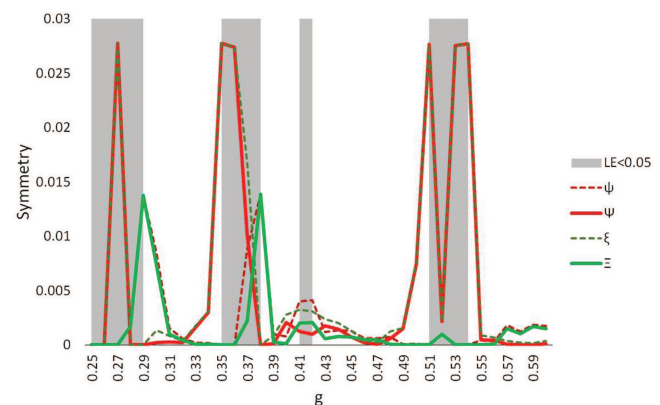
**FIG. 4.** The phase diagrams for  $g = 0.27$  (left) and  $g = 0.29$  (right), showing the physical phenomena which lead to rotational and mirror symmetry, respectively. Note the three  $x$  axis crossings at  $g = 0.27$ , signifying a period-3 orbit, and the rough vertical symmetry of  $g = 0.29$ , showing geometrical, if not topological, time-reversibility.

$$\Xi = \frac{(\bar{P}_{M1} - \bar{P}_{all})^2 + (\bar{P}_{M2} - \bar{P}_{all})^2 + (\bar{P}_{M3} - \bar{P}_{all})^2}{3}. \quad (14)$$

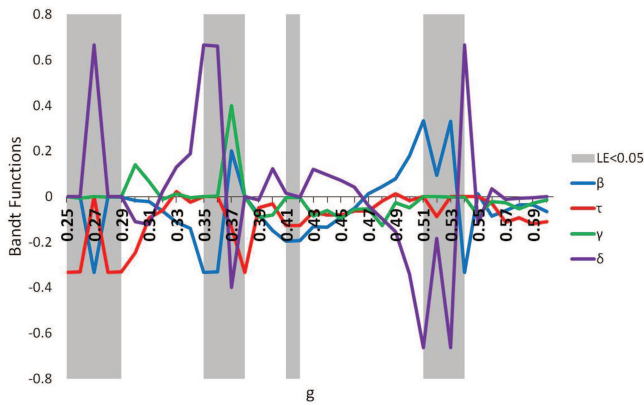
Rotational variance tracks the variance of each word relative to the average of its rotational symmetry group, and mirror variance does the same with mirror symmetry groups. Likewise, rotational hierarchy measures the variance of each rotational symmetry group's average population against the average for all six words; similarly, mirror hierarchy measures each mirror symmetry group average. That is to say, if the population of certain words agree with other words in their symmetry group, then variance,  $\psi$  or  $\xi$ , will be low. If the system has a clear preference for one symmetry group over others, then the hierarchies,  $\Psi$  or  $\Xi$ , will be high.

Figure 5 quantifies these symmetries as a function of the control parameter  $g$ . In it, we can appreciate how chaotic regions in which words are somewhat ordered, such as 0.34 and 0.50, have significantly higher hierarchy and lower variance in one type of symmetry than in other chaotic regions (the latter, therefore, being arguably “truly” chaotic). Stable regions ( $LE < 0$ ) have even higher hierarchy. This brings home the significance of our result that—at least on the basis of this exploration of the Duffing oscillator—by measuring the symmetry of the dynamics, we can conclude that the existence of a rotational or mirror hierarchy value between 0.002 and 0.007 or greater signifies the existence of stable parameter regimes in the neighborhood (thus, this is “pre-stable chaos”), while hierarchy values closer to 0.01 or greater represents true stability.

The advantage of this grouping and quantifying words this way is that, if any meaningful underlying order in the words increases near stability, it would be shown through these measures more clearly, and numerically, than by judging word populations by eye. The philosophy is similar to that of Bandt's work<sup>18</sup> on functions



**FIG. 5.** Plot of symmetry measures as a function of  $g$ . Because of the orthogonality of rotational and mirror symmetry groups, rotational variance often agrees with mirror hierarchy, likewise rotational hierarchy and mirror variance. However, each variance is never less than the opposite hierarchy.



**FIG. 6.** Plot of Bandt's functions as a function of  $g$ , with stable  $g$ -values highlighted in gray. In the symmetries of Fig. 5, note the increase in one hierarchy, at 0.30, 0.34, and 0.50, relative to their chaotic neighbors. Similarly, in Bandt's functions, the absolute values of up–down measures  $\beta$  and  $\delta$  increase at the same points.

defined as

$$\beta = P_{012} - P_{210}, \quad (15)$$

$$\tau = P_{012} + P_{210} - \frac{1}{3}, \quad (16)$$

$$\gamma = P_{102} + P_{120} - P_{021} - P_{201}, \quad (17)$$

$$\delta = P_{021} + P_{102} - P_{120} - P_{201}, \quad (18)$$

where  $\beta$  is termed up–down balance,  $\tau$  is persistence,  $\gamma$  is rotational asymmetry, and  $\delta$  is up–down scaling. There is a clear correspondence between the physical significance of Bandt's  $\gamma$  and our  $\xi$ , as time-reversal asymmetries, although Bandt names  $\gamma$  as “rotational asymmetry.” Thus, symmetry measures (specifically either  $\Psi$  and  $\psi$  or  $\Xi$  and  $\xi$ ) and Bandt's functions condense word population information into a more concise, readable set of statistics, which are distinct from PE, and are useful in tracking temporal orderings and structure in the dynamics. In Fig. 6, we see the functions introduced by Bandt in Ref. 18. Compared to what we see in Fig. 5, the Bandt measures seem unable or only weakly to discern dynamical transitions, at least in this complex system—that is, there is an increase or decrease of  $\beta$  or  $\delta$  in the chaotic regime right before  $g = 0.35$  and  $g = 0.51$ , but there is no visible change right after  $g = 0.29$  or  $g = 0.38$ .

In Fig. 5, we see correlation of increased symmetry (as measured by  $\Xi$ ,  $\Psi$ ) as a function of  $g$  with neighboring chaos-stability transitions (in LEs or PEs), but this is imperfect, as false negative and false positive signals of nearby stability do occur. Explorations of the same quantities as above with variation in other parameters such as  $\omega$  (not shown) also confirm this pattern of words always being ordered in the stable regime, as shown in Figs. 1 and 3, but only being ordered within the chaotic regime typically near an upcoming transition to regularity. To quantify this “typicality” of correlation in the parameter neighborhood between symmetry and dynamical stability, we compute the quantities defined below, and shown in Fig. 7.

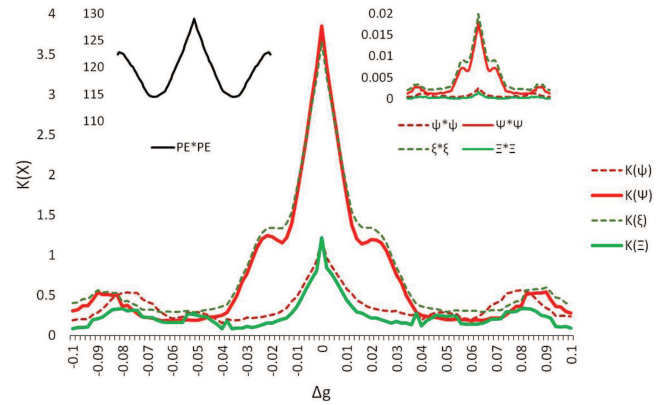


**FIG. 7.** The controlled cross-correlation of the permutation entropy with the symmetry measures, across offset  $\Delta g$ , along with auto-correlations for PE (left inset) and all symmetry measures (right inset). The horizontal range ( $\Delta g$ ) of the insets is the same as that of the main figure. The local minima around  $\pm 0.015$  for  $\Psi$  indicate that rotational symmetry increases near low permutation entropy with an offset of  $|\Delta g| \approx 0.015$ . This means that we can anticipate a chaos-stability shift in parameter space using symmetry measures and succeed with some reliability.

We seek to measure the degree to which the functions  $PE(g)$  and  $X(g) - X$  being a general form of the measures  $\xi$ ,  $\Xi$ ,  $\psi$ ,  $\Psi$ —overlap, including as  $X(g)$  is shifted  $\Delta g$  with respect to  $PE(g)$ . That is, does an increase in a symmetry measure indeed quantifiably correlate with a neighboring shift in  $PE$  from chaos to regularity? If so, this would indicate that the information contained in the dynamical system for a specific value of  $g$  is consistent with its dynamics at a neighboring value of  $g$ , even across a chaos-stability transition. Because this information is accessed through symmetry measures, it would also mean that symmetry measures have *quantifiable* power in predicting chaos-stability shifts.

We first compute the auto-correlation of each symmetry  $X \star X$  with itself. We do the same for the PE. These are shown in the insets of Fig. 7 as functions of the parameter offset  $\Delta g$ . The general form of a correlation integral across  $g$  is given below

$$x(g) \star y(g) = \int x(g + \Delta g) y(g) dg. \quad (19)$$

To account for the finite range in  $g$ , we take repeating boundary conditions; that is, for both factors in the correlation functions, we wrap around the standard  $g$ -range of  $0.25 \leq g \leq 0.60$ , with the offset  $\Delta g$  determining where the two functions overlap. Of course, this results in an artificial increase in the auto-correlation/self-overlap as  $|\Delta g|$  gets very large, with edge-effects visible at  $\Delta g = \pm 0.175$ . To suppress the false signal from this artificial effect, we consider correlations only for  $|\Delta g| < 0.1$ .

We see in the auto-correlations that PE has self-agreement (peaks) at offsets of about  $|\Delta g| \approx 0.10$ , which makes sense given the apparent average size of the chaos-stability windows shown in Figs. 1 and 2. Symmetries show the same, though smaller peaks at  $|\Delta g| \approx 0.09$  and also anti-correlations (a local minimum in the correlation function). Specifically, the rotational hierarchy  $\Psi$  is moderately anti-correlated with itself at an offset of  $|\Delta g| \approx 0.015$ ,

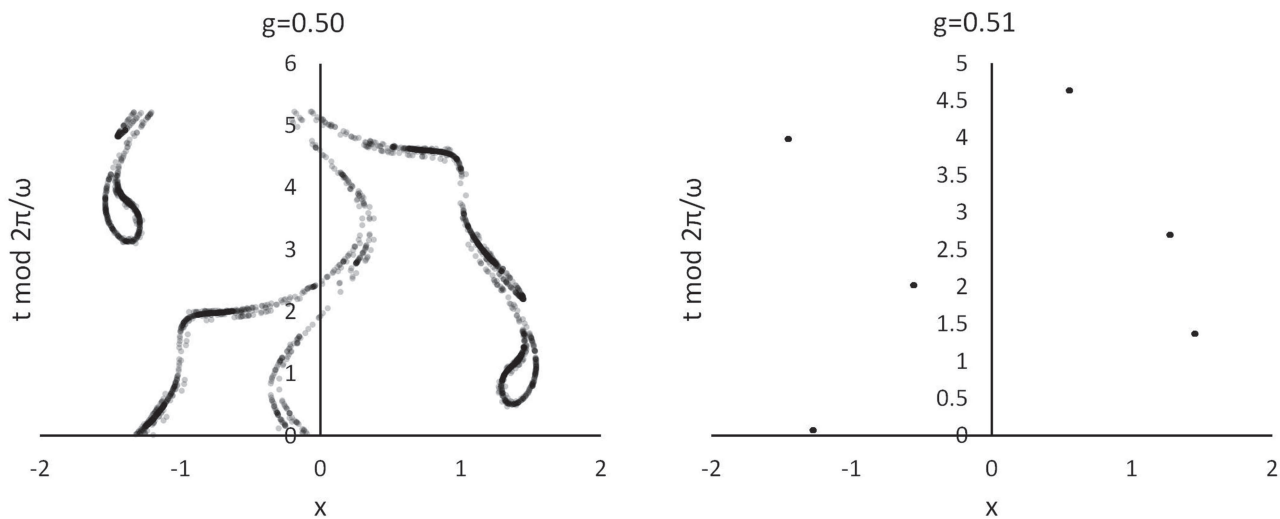


**FIG. 8.** The generalized Poincaré sections for  $g$ -values 0.50 and 0.51. The implied time-delayed symmetry at  $g = 0.50$  is a result of the fact that GPS takes data at both peaks and valleys in the time-series. Although few points are visible at  $g = 0.51$ , the amount of information depicted is roughly equal to that of  $g = 0.50$ , greater than 1500 data points each. At  $g = 0.50$ , the LE is positive, while at  $g = 0.51$ , it is zero.

and its autocorrelation falls to zero at offsets  $|\Delta g| \approx 0.05$ . This anti-correlation is consistent with symmetries increasing between chaos and stability, with chaotic and stable windows being, on average,  $0.05 = |\Delta g|$  away from each other.

Finally, we construct a “controlled” Cross Correlation  $K$  between the PE and all the Symmetries  $X$ , which includes compensating for auto-correlation scales for the PE and Symmetries:

$$K(X) = \frac{(PE \star PE)(X \star X)}{PE \star X}. \quad (20)$$

This is the central graph in Fig. 7. Note that at an offset of  $\Delta g \approx \pm 0.015$  there are local minima in  $\Psi \star \Psi$  and  $K(\Psi)$ , indicating that  $\Psi$  disagrees with the PE especially at these values. That is, increases in  $\Psi$  at one  $g$ -value correlate to decreases in PE at a  $g$ -value lesser or greater by 0.015, and thus the behavior of the symmetry in word populations is correlated—albeit weakly—with nearby chaos-stability shifts. This “dip” at  $\Delta g \approx 0.015$  is exactly consistent with our visual observations and discussions above. To the best of our knowledge, this is a novel instance of an ability to “peer around the corner” in parameter space to identify chaos-stability transitions.

#### IV. COMPARISON WITH OTHER MEASURES

To understand whether this potential ability to “peer around the corner” at the existence of stable behavior at a *neighboring* parameter is visible in other more standard measures and diagnostics, we have compared what we see in the word populations with a variety of some of the most common tools used to distinguish between chaos and regularity. Specifically, we have considered if such behaviors are visible in Poincaré sections (PSs), and Fourier

transforms (FTs). PS can be of various sorts, but for a driven system it measures the position and momentum of a system stroboscopically at regular intervals determined by the system’s natural frequency. It is also typical to use Fourier transforms on observational time-series to characterize the dynamics via its spectral decomposition. While we do not report details, neither of these showed the sort of distinct change in behavior visible in word populations, and so we searched further in order to understand if variations on the standard diagnostics might better help us understand our results in the previous section. To this end we developed (somewhat) new quantifiers aimed at getting more direct insight into the temporal behavior of interpeak interval, specifically Generalized Poincaré Sections (GPSs) and Interval Trio Maps (ITMs). Generalized Poincaré Sections (GPSs), like normal PS, represent the intersections of the trajectory with a plane in phase-space; in this case, unusually for a driven system, we record  $x[t]$  and  $t \bmod \frac{2\pi}{\omega}$  values whenever  $p[t]$  equals zero (as opposed to using a certain phase for the sinusoidal driving for recording  $x$  and  $p$ ). This is merely a rotation of perspective on the trajectory: instead of displaying place and speed at regular time, it shows place and time at regular speed. The relevance of shifting to this GPS is that it records time values at peaks and valleys of the oscillator, thus recording in fact the same sort of information as used to construct interpeak words, and thus arguably liable to show similar behavior.

Similarly, interval trio maps track interpeak intervals much like words, but display numerical information, rather than merely ordinal. That is, an ITM is a 3-dimensional representation of trios of consecutive interpeak intervals: every trio is a point in interval-space, where each dimension of that space represents the length of the corresponding interval in the trio. The interval-space of ITMs is divided by three diagonal planes, where two intervals are of equal length: 1st–2nd, 1st–3rd, and 2nd–3rd, equivalent to the planes

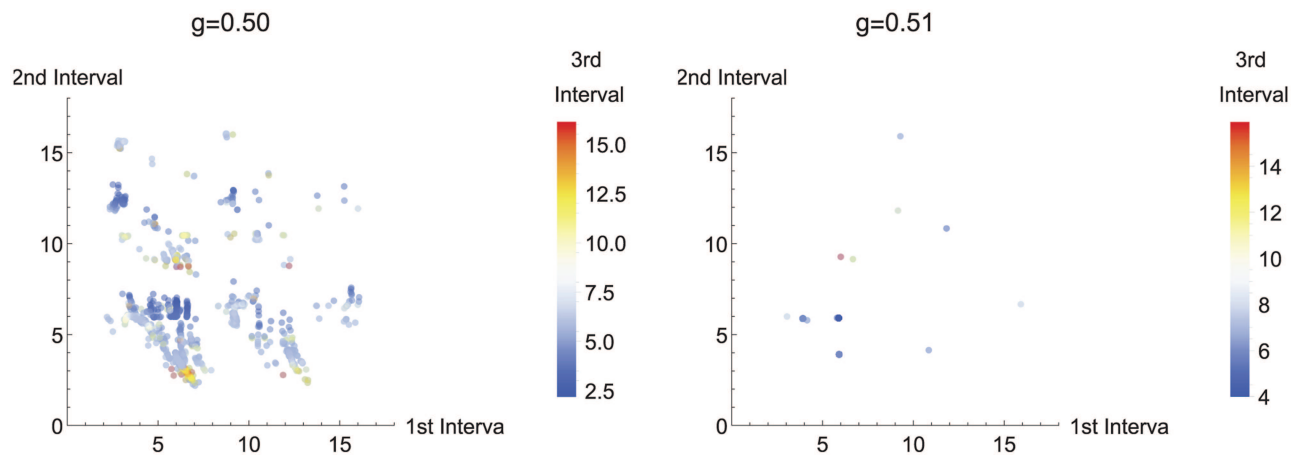


**FIG. 9.** The Interval Trio Maps for  $g$ -values 0.50 (positive LE, i.e., chaotic) and 0.51 (zero LE, i.e., regular) as a function of the first two interval. The third interval is represented by color, with warm colors corresponding to longer third intervals.

defined by the equations

$$x = y, x = z, y = z. \quad (21)$$

These diagonal planes divide ITMs into six sectors (similar to octants, but only six because the three planes are not orthogonal), with every point in each sector mapping to an instance of an ordinal pattern or word such that the population associated with a given word amounts to the count of points in a given sector.

We used the same time-series data across the same range of  $g$  for ITMs (see Fig. 9) and for GPSs (see Fig. 8) as for word populations. We find that indeed ITMs (as shown), LEs, and PSs, as well as GPSs (as shown), all behave similarly with regard to chaos-stability shifts, in that they show the presence or absence of chaos as a binary—that is, whether or not there is chaos. This is in contrast to the acute sensitivity visible in word populations that quantifies greater and lesser degrees of chaos and different types of stability (even at the same LEs). This is significant because it means that words show a type of structural distinction that is invisible to other metrics. The ITM and GPS both exhibit visual changes that can be described qualitatively as a cloudiness or smearing at the same  $g$ - and  $w$ -values as the PS, with small, gradual changes of shape across chaotic zones. PS, because they project a large number of data points across a phase space rather than condensing their information into a single number, contains rather more information, but this information often becomes obscured behind subtle changes, and again, the clearest indicator—the smearing effect—only indicates the presence or absence of chaos and perhaps the size and range of the attractor at a given system parameter. This agreement between GPS and PS is expected, albeit less interesting than if they had disagreed in some way.

ITMs contain strictly more information than words (because words can be directly derived from ITMs, but not vice versa) but do not *noticeably* show this sensitivity to greater or lesser degrees of chaos, which may initially be puzzling. However, more careful

analysis of the ITMs allows a little more insight into what we have observed. In particular, smooth changes in the ITMs which do not visibly alter it can sometimes yield drastic changes in word populations. This is because which word an interval trio belongs to is dependent on its location as a point in interval-space and continuous changes in location can map to discrete changes in which sector to which words are assigned. As a cusp example, if an Interval Trio is on or near the boundaries that coincides with all three planes, then all three intervals are of equal length and the word created is  $w_{111}$ , but a small deviation from this equality by any two of the three intervals could move the point into one of the six sectors. Thus, word population changes amount to changes in higher-order correlations in the statistics of ITMs, and the ordinalization (and data compression) implicit in analyzing word populations allows us to pick out the effects of slight regime changes in the high-order properties of ITMs. This effect seems to be how word-derived measures provide an advantage in predicting stability in nearby parameter regimes for a system otherwise only understood as being chaotic, and this advantage is what we observe via the symmetry measures.

## V. CONCLUSION

To summarize, we have investigated the parameter dependence of chaos and stability and transitions between the two for the Duffing oscillator by computing a variety of measures, including words as a function of parameter. In our study, word populations, and their derived symmetry measures, are seen to be visibly sensitive to regime changes within and between stability and chaos, beyond the blunt binary measures (of chaos or stability) displayed by the LE, PS, FT, and ITM. At least for this system, an observed increase in symmetry measures signals an increased chance of success if we search for regular behavior at nearby parameter values, even though this is not a causal measure. That is, word population symmetry analysis can be used to “peer around the corner” to anticipate a change in dynamics in the parameter space.

It might seem that by selecting only certain events from a time-series we lose information about the system dynamics. However, as all analysis dependent on this ordinalization of data shows, this sort of compression to events provides efficient and necessary indicators of the structure of the dynamics. This is what happens when projecting Poincaré sections, for example. On the other hand, we have also seen that something like the PE seems to compress the data so much as to lose other valuable information. Furthermore, of course, this technique can be specially useful in analyzing experimental data. It is relatively difficult to compute the LE in those cases, and moreover, word populations are robust to unavoidable experimental noise.

We argue that this weak correlation is a real and valuable effect by considering thought experiments in practical situations with such chaos-stability transitions. The correlation found between word symmetries in chaos and nearby stability would be a tangible advantage. If, for instance, engineers seek to stabilize a bridge against chaos in the presence of small increase in traffic or driving amplitude, an LE or PS, or even an FT, would only say whether the current oscillations are chaotic or not. Words, on the other hand, have symmetries whose presence correlates with nearby stability and so could help signal the appropriate change in other system parameters. Examples would be the ability to provide changed predictive abilities for systems such as precipitation patterns under climate change,  $N$ -body gravitational problems with non-constant masses, and bridges swaying under varying amounts of traffic or wind.

The limits and conditions for the utility of word analyses, especially as predictors of chaos-stability transitions remain to be tested more widely. Other than testing other dynamical systems, of course, we also need to consider how the observed correlation between word symmetries and stability behaves in a higher-dimensional parameter space, including the possible role of the resolution in the parameter space that allows us to pick out these correlations. Other factors which may be need to understand include the role of the minimum resolution for time in the time-series, below which periodic words grow so populous that hierarchalizing interpeak intervals becomes inefficient. Despite these open questions, it is clear that exploring word populations in dynamical time-series continues to yield a surprising wealth of information about a system's dynamics.

## ACKNOWLEDGMENTS

We wish to acknowledge internal support at Carleton College for funding student research.

## DATA AVAILABILITY

The data that support the findings of this study are available from any of the authors upon reasonable request.

## REFERENCES

- <sup>1</sup>G. Boffetta *et al.*, "Predictability: A way to characterize complexity," *Phys. Rep.* **356**(6), 367–474 (2002).
- <sup>2</sup>T. Shinbrot, C. Grebogi, J. A. Yorke, and E. Ott, "Using small perturbations to control chaos," *Nature* **363**, 411–417 (1993).
- <sup>3</sup>S. Hayes, C. Grebogi, and E. Ott, "Communicating with chaos," *Phys. Rev. Lett.* **70**, 3031 (1993).
- <sup>4</sup>H. L. D. de S. Cavalcante, M. Oriá, D. Sornette, E. Ott, and D. J. Gauthier, "Predictability and suppression of extreme events in a chaotic system," *Phys. Rev. Lett.* **111**, 198701 (2013).
- <sup>5</sup>L.-Z. Wang, R.-Q. Su, Z.-G. Huang, X. Wang, W.-X. Wang, C. Grebogi, and Y.-C. La, "A geometrical approach to control and controllability of nonlinear dynamical networks," *Nat. Comm.* **7**, 11323 (2016).
- <sup>6</sup>A. Wolf *et al.*, "Determining Lyapunov exponents from a time series," *Physica D* **16**(3), 285–317 (1985).
- <sup>7</sup>C. Bandt and P. Bernd, "Permutation entropy: A natural complexity measure for time series," *Phys. Rev. Lett.* **17**, 1–4 (2002).
- <sup>8</sup>J. Amigó *et al.*, "Order patterns and chaos," *Phys. Lett. A* **355**, 27–31 (2006).
- <sup>9</sup>J. Amigó, "Detection of determinism," in *Permutation Complexity in Dynamical Systems* (Springer, Berlin, 2010), pp. 147–158.
- <sup>10</sup>Y. Zou, R. V. Donner, N. Marwan, J. F. Donges, and J. Kurths, "Complex network approaches to nonlinear time series analysis," *Phys. Rep.* **787**, 1–97 (2019).
- <sup>11</sup>M. L. Trostel, M. Z. R. Misplon, A. Aragonese, and A. K. Pattanayak, "Characterizing complex dynamics in the classical and semi-classical duffing oscillator using ordinal patterns analysis," *Entropy* **20**, 40 (2018).
- <sup>12</sup>M. Barreiro, A. C. Marti, and C. Masoller, "Inferring long memory processes in the climate network via ordinal pattern analysis," *Chaos* **21**, 013101 (2011).
- <sup>13</sup>M. C. Soriano, L. Zunino, O. A. Rosso, I. Fischer, and C. R. Mirasso, "Time scales of a chaotic semiconductor laser with optical feedback under the lens of a permutation information analysis," *IEEE J. Quant. Elec.* **47**(2), 252 (2011).
- <sup>14</sup>U. Parlitz, S. Berg, S. Luther, A. Schirdewan, J. Kurths, and N. Wessel, "Classifying cardiac biosignals using ordinal pattern statistics and symbolic dynamics," *Comput. Biol. Med.* **42**, 319–327 (2012).
- <sup>15</sup>G. Tirabassi and C. Masoller, "Unravelling the community structure of the climate system by using lags and symbolic time-series analysis," *Sci. Rep.* **6**, 29804 (2016).
- <sup>16</sup>M. Colet and A. Aragonese, "Forecasting events in the complex dynamics of a semiconductor laser with optical feedback," *Sci. Rep.* **8**, 210741 (2018).
- <sup>17</sup>J. Guckenheimer and P. Holmes, *Nonlinear Oscillations, Dynamical Systems and Bifurcations of Vector Fields* (Springer, 1983).
- <sup>18</sup>C. Bandt, "Permutation entropy and order patterns in long time series," in *Time Series Analysis and Forecasting, Contributions to Statistics*, edited by I. Rojas and H. Pomares (Springer, 2015).
- <sup>19</sup>C. Bandt, "Small order patterns in big time series: A practical guide," *Entropy* **21**(6), 613 (2019).